Distributed Sensor Coordination Algorithms for Efficient Coverage in a Network of Heterogeneous Mobile Sensors

Hamid Mahboubi, Kaveh Moezzi, Amir G. Aghdam and Kamran Sayrafian-pour

***Abstract*—The main focus of this work is directed towards distributed coordination algorithms for coverage in a mobile sensor network. The sensors are assumed to have nonidentical sensing ranges, and it is desired to move them in such a way that the total sensing coverage increases as much as possible. To this end, the field is partitioned using the multiplicatively weighted Voronoi cells, and then different geometric methods are developed to find new locations for the sensors such that the coverage is improved. The proposed algorithms are iterative, and use the available local information to place the sensors properly, aiming to reduce the size of the coverage holes in the network. Simulations demonstrate the good performance of the proposed algorithms.**

I. Introduction

Wireless sensor networks have received a great deal of attention in the past decade, and have found a broad range of applications in various areas [1], [2], [3]. Examples of sensor network applications include biomedical engineering, security surveillance, target tracking and environmental monitoring, to name only a few [4], [5], [6]. In particular, a mobile sensor network (MSN) is comprised of a number of wireless nodes, where each node is capable of moving in different directions and communicating with a subset of sensors in order to achieve a global objective. Typical objectives in a mobile sensor network includes monitoring of a moving target [7] and energy-efficient area coverage [8]. In practice, to achieve the desired goals cooperatively, it is often preferable to use a decentralized decision-making scheme for sensor deployment [9]. Furthermore, the deployment strategy needs to be independent of the initial location of the sensors, as such information is usually unavailable [10]. In addition, the cost-effective resource management techniques are required to prolong the network lifetime [11].

In this paper, three distributed deployment algorithms are presented for a network of nonidentical sensors. The multiplicatively weighted Voronoi (MW-Voronoi) diagram is employed to detect coverage holes, where each sensor weight is proportional to its sensing range [12]. The algorithms are called farthest point boundary (FPB), Maxmin-vertex and Minmax-vertex. The main characteristic of these algorithms is that they are distributed and perform iteratively. Furthermore, once each destination is computed and before the sensor moves, its local coverage area (defined later) from the new location is compared to the current value, based on which the sensor either moves to the new location or stays in its current position. In this paper, novel geometric techniques are developed to find the optimal location of sensors for maximizing coverage area in a mobile sensor network, where convex optimization techniques cannot solve the problem.

The reminder of the paper is planned as follows. In Section II, some background information as well as important notions and definitions is presented. Section III provides new sensor deployment algorithms to increase sensing coverage, as the main contribution of this paper. Simulations are presented in Section IV, and finally conclusions are summarized in Section V.

II. Preliminaries

Let $\mathbf{S}$ be a set of n distinct weighted nodes in the plane denoted by $(S_1, w_1), (S_2, w_2), \ldots, (S_n, w_n)$, where $w_i > 0$ is the weighting factor associated with S_i, for any $i \in \mathbf{n} := \{1, 2, \ldots, n\}$. It is desired now to partition the plane into n regions such that:

- Each region contains only one node, called its generating node, and
- the nearest node, in the sense of weighted distance, to any point inside a region is the generating node of that region.

The diagram obtained by the partitioning described above is called the *multiplicatively weighted Voronoi diagram* (MW-Voronoi diagram) [12]. Analogous to conventional Voronoi diagram, the mathematical characterization of each region obtained by the partitioning described above is as follows:

$$\Pi_i = \left\{ Q \in \mathbb{R}^2 \mid w_j d(Q, S_i) \leq w_i d(Q, S_j), \forall j \in \mathbf{n} \backslash \{i\} \right\} \tag{1}$$

for any $i \in \mathbf{n}$, where $d(Q, S_i)$ is the Euclidean distance between Q and S_i.

Some of the following definitions and assumptions are borrowed from [13].

Definition 1. Sensors i and j are said to be neighbors if $\Pi_i \cap \Pi_j \neq \emptyset$, i.e., their MW-Voronoi regions share some points on their boundaries. Denote the set of neighboring sensors of sensor i by $\mathbf{N}_i$.

Definition 2. Consider the sensor S_i with the sensing radius r_i and the corresponding MW-Voronoi region Π_i, $i \in \mathbf{n}$, and let Q be an arbitrary point inside Π_i. The intersection of the region Π_i and a circle of radius r_i centered at Q is referred to as the *i-th coverage area w.r.t. Q*, and is denoted by $\beta^Q_{\Pi_i}$. The

H. Mahboubi is with the Harvard John A. Paulson School of Engineering and Applied Sciences, 29 Oxford Street, Cambridge, MA 02138 USA, mahboubi@seas.harvard.edu

K. Moezzi is with the Pratt & Whitney Canada, 1000 Boulevard Marie-Victorin, Longueuil, Québec J4G 1A1 Canada, kavehmoezi@yahoo.com

A. G. Aghdam is with the Department of Electrical & Computer Engineering, Concordia University, 1455 de Maisonneuve Blvd. W., EV012.179, Montréal, Québec H3G 1M8 Canada, aghdam@ece.concordia.ca

K. Sayrafian-Pour is with the National Institute of Standards and Technology (NIST), 100 Bureau Drive, Stops 8920 Gaithersburg, MD 20899 USA ksayrafian@nist.gov

This work has been supported by the National Institute of Standards and Technology (NIST), under grant 70NANB8H8146.

i-th coverage area w.r.t. the location of the sensor S_i is called the *i-th local coverage area* of that sensor, and is denoted by β_{Π_i}.

Definition 3. Consider an arbitrary point Q inside the MW-Voronoi region Π_i, $i \in \mathbf{n}$. The set of all points in Π_i which do not belong to $\beta^Q_{\Pi_i}$ is referred to as the *i-th coverage hole w.r.t Q*, and is denoted by $\theta^Q_{\Pi_i}$. The i-th coverage hole w.r.t. the location of the sensor S_i is called the *i-th local coverage hole* of that sensor, and is denoted by θ_{Π_i}. Also, the union of all local coverage holes, denoted by θ, is called the *total coverage hole*, i.e. $\theta = \sum_{i=1}^{n} \theta_{\Pi_i}$.

Definition 4. [14] The *Apollonian circle* of the segment AB, denoted by $\Omega_{AB,k}$, is the locus of all points E such that $\frac{AE}{BE} = k$.

The MW-Voronoi diagram is used in this work to develop sensor deployment algorithms. Every sensor has a circular sensing area whose size is not the same for all sensors. Consider each sensor as a weighted node whose weight is equal to its sensing radius, and draw the MW-Voronoi diagram. It is a straightforward results of (1) that if a sensor cannot detect a phenomenon in its region, there is no other sensor that can detect it either. This implies that to find the coverage holes in the sensing field, it would suffice to compare the MW-Voronoi region of every node with its local coverage area.

Notation 1. Consider a circle of radius r centered at O, denoted hereafter by $\Omega(O, r)$, and a point V in the plane. The intersection of Ω and the extension of VO from O is denoted by $T^V_{\Omega(O,r)}$. The other intersection point of $\Omega(O, r)$ and VO (or its extension) is denoted by $\bar{T}^V_{\Omega(O,r)}$.

Notation 2. As mentioned before, the boundary curves of an MW-Voronoi region are the segments of some Apollonian circles. The set of all such Apollonian circles for the i-th MW-Voronoi region is denoted by $\mathbf{\Omega}_i$. The sets $\bar{\mathbf{\Omega}}_i$ and $\tilde{\mathbf{\Omega}}_i$ are defined as follows:

$$\bar{\mathbf{\Omega}}_i = \{\Omega \in \mathbf{\Omega}_i | S_i \in \Omega\}$$
$$\tilde{\mathbf{\Omega}}_i = \{\Omega \in \mathbf{\Omega}_i | S_i \notin \Omega\}$$

Assumption 1. [13] The graph representing the communication topology of sensors is connected [15]. This means that every sensor can obtain the information required to construct its MW-Voronoi region.

III. Sensor Deployment Strategies

Three different distributed sensor coordination techniques are developed in this section for a mobile sensor network. The algorithms are iterative, similarly to [16], where every sensor S_i, $i \in \mathbf{n}$, first broadcasts its location P_i and sensing radius r_i to its neighboring sensors, and then constructs its MW-Voronoi region Π_i using the similar information it receives from them. It then checks for possible coverage holes in the region. If a coverage hole is detected, the sensor finds a target position (but does not move there) such that by moving there the coverage hole would be eliminated, or its size would be reduced by at least a certain amount. Let the new target position for sensor S_i, $i \in \mathbf{n}$, be denoted by $\acute{P}_i$, and find $\beta^{\acute{P}_i}_{\Pi_i}$, i.e., the coverage area w.r.t. the new position. If this area is greater than the current local coverage area (note that the sensor has not moved yet), i.e. $\beta^{\acute{P}_i}_{\Pi_i} > \beta^{P_i}_{\Pi_i}$, the sensor moves to the new position; otherwise, it stays in its current location. The algorithm stops when the coverage increase by each sensor in two consecutive iterations does not exceed a prescribed value.

The following theorem is similar to Theorem 1 of [16], and shows that the total coverage under the sensor deployment scheme described in the previous paragraph always increases.

Theorem 1. *Consider a set $\mathbf{S}$ of n sensors in the plane with their positions and sensing radii denoted by the sets $\mathbf{P} = \{P_1, P_2, \ldots, P_n\}$ and $\mathbf{r} = \{r_1, r_2, \ldots, r_n\}$, respectively, and let the MW-Voronoi regions be $\Pi_1, \Pi_2, \ldots, \Pi_n$. Assume the sensors move to new positions $\acute{\mathbf{P}} = \{\acute{P}_1, \acute{P}_2, \ldots, \acute{P}_n\}$, where $\acute{P}_i \neq P_i$ for all i belonging to $\mathbf{K}$, a non-empty subset of $\mathbf{n}$ (note that the MW-Voronoi regions corresponding to the position set $\acute{\mathbf{P}}$ will be different from $\Pi_1, \Pi_2, \ldots, \Pi_n$). If the i-th coverage area w.r.t. $\acute{P}_i$ in the previously constructed MW-Voronoi region Π_i is greater than the i-th local coverage area in Π_i (i.e., $\beta^{\acute{P}_i}_{\Pi_i} > \beta^{P_i}_{\Pi_i}$) for all $i \in \mathbf{K}$, then the total coverage increases.*

Proof: The proof is similar to that of Theorem 1 in [16]. ■

Notation 3. An MW-Voronoi diagram with n regions $\Pi_1, \Pi_2, \ldots, \Pi_n$ will hereafter be represented by $\mathcal{V}$, and the number of vertices of region Π_i will be denoted by m_i, for any $i \in \mathbf{n}$.

A. Farthest Point Boundary Strategy (FPB)

In this algorithm, each sensor moves toward the farthest point in its MW-Voronoi region such that any existing coverage hole in its region can be covered. This point is denoted by $X_{i,far}$ for the i-th region. In fact, once a sensor detects a coverage hole, it calculates the farthest point (using the information about its MW-Voronoi region as well as the coverage holes in that region, as it will be shown later) and moves toward it continuously until $X_{i,far}$ is covered. The following definition is used to calculate the farthest point in each MW-Voronoi region.

Definition 5. The corner points of the i-th MW-Voronoi region (i.e., the intersection of its boundary curves) are denoted by $V_{i1}, V_{i2}, \ldots, V_{im_i}$. These points will hereafter be referred to as the MW-Voronoi vertices for the i-th MW-Voronoi region (note that a region may have no vertex). It is to be noted that the farthest point in each MW-Voronoi region lies on the boundary of the region.

Theorem 2. *Let $\mathbf{A}_i$ be the set of all vertices for the i-th region ($i \in \mathbf{n}$) of the MW-Voronoi diagram $\mathcal{V}$, and define the set $\mathbf{B}_i$ as follows:*

$$\mathbf{B}_i = \left\{ T^{S_i}_{\Omega_{S_i S_j, k}} \mid k = \frac{w_i}{w_j},\ 1 \leq j \leq n,\ S_j \in \mathbf{N}_i \right\}$$

where $\mathbf{N}_i$ is the set of all neighbors of the i-th sensor. Then the farthest point in the i-th region belongs to the union of the sets $\mathbf{A}_i$ and $\mathbf{B}_i$; i.e., $X_{i,far} \in \mathbf{A}_i \cup \mathbf{B}_i$.

Proof: As noted earlier, $X_{i,far}$ lies on the boundary of the i-th region. Consider the following two cases:
Case 1: $X_{i,far}$ is on the boundary curve $V_{i1}V_{i2}$ such that $V_{i1}V_{i2} \in \Omega_{S_i S_g, \frac{w_i}{w_g}}$. If $T^{S_i}_{\Omega_{S_i S_g, \frac{w_i}{w_g}}}$ is on the boundary curve

$V_{i1}V_{i2}$, given that for any positive $\frac{w_i}{w_g} \neq 1$, $T^{S_i}_{\Omega_{S_iS_g,\frac{w_i}{w_g}}}$ is the farthest point to S_i and S_g, thus $X_{i,far} \in \mathbf{B}_i$; otherwise, since among all points on the boundary curve $V_{i1}V_{i2}$ either V_{i1} or V_{i2} is the nearest point to $T^{S_i}_{\Omega_{S_iS_g,\frac{w_i}{w_g}}}$, hence $X_{i,far}$ is either V_{i1} or V_{i2}. This means that $X_{i,far} \in \mathbf{A}_i$.
Case 2: $X_{i,far}$ is on the boundary segment $V_{i3}V_{i4}$. In this case, it is straightforward to show that the farthest point is either V_{i3} or V_{i4}. This means that $X_{i,far} \in \mathbf{A}_i$.
Therefore, in both cases considered above $X_{i,far} \in \mathbf{A}_i \cup \mathbf{B}_i$. ■

Note that according to Theorem 2, the farthest point of the i-th MW-Voronoi region belongs to a set of points with $2 \times dim(\mathbf{N}_i)$ elements.

B. Maxmin-Vertex Strategy

The main idea of the Maxmin-vertex strategy is based on the fact that normally for a good coverage result, the sensors should not be too close to the vertices of their MW-Voronoi regions. In this strategy, the target position of each sensor in every iteration is selected as a point inside its MW-Voronoi region with maximum distance from the nearest vertex. This point is denoted by $\bar{O}_i$ for the i-th MW-Voronoi region, $i \in \mathbf{n}$, and is called the *Maxmin-vertex centroid*. Denote the distance between $\bar{O}_i$ and the nearest vertex to it by $\bar{r}_i$.

Definition 6. The Maxmin-vertex circle of a region in the MW-Voronoi diagram $\mathcal{V}$ is defined as the largest circle centered inside that region such that all of the vertices of the region are either outside the circle, or on it. This circle is, in fact, $\Omega(\bar{O}_i, \bar{r}_i)$ for the i-th region ($i \in \mathbf{n}$).

Lemma 1. *Suppose the i-th MW-Voronoi region is not a circle (i.e., it has at least two boundary curves). If the Maxmin-vertex circle passes through exactly one vertex, say V_{i1}, then $\bar{O}_i$ is $T^{V_{i1}}_{\Omega}$ for some $\Omega \in \mathbf{\Omega}_i$; otherwise, the circle passes through more than one vertex.*

Proof: Let $\bar{V}_{i1}$ be the nearest vertex of the i-th MW-Voronoi region to $\bar{O}_i$, and define:

$$\hat{u} := \min_{V \in \mathbf{V}_i - \{\bar{V}_{i1}\}} \left\{ d(\bar{O}_i, V) \right\}, \quad i \in \mathbf{n} \tag{2}$$

where $\mathbf{V}_i$ is the set of vertices of the i-th MW-Voronoi region in the MW-Voronoi diagram.

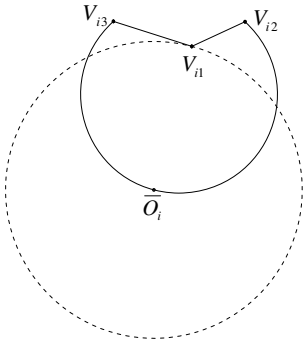

Fig. 1: An example of the Maxmin-vertex circle, when it passes through exactly one vertex.

Suppose $\bar{O}_i$ and $T^{\bar{V}_{i1}}_{\Omega}$ are disjoint for any $\Omega \in \mathbf{\Omega}_i$. Suppose also that the Maxmin-vertex circle does not pass through any vertex other than $\bar{V}_{i1}$, and hence the parameter $\delta^* = (\hat{u} - \bar{r}_i)/2$ is strictly positive. There are two possible cases, as discussed below.
Case 1: $\bar{O}_i$ is inside the i-th MW-Voronoi region. Let $\hat{O}$ be a point inside the i-th MW-Voronoi region and on the line $\bar{V}_{i1}\bar{O}_i$, but closer to $\bar{O}_i$, such that the distance between $\bar{O}_i$ and $\hat{O}$ is equal to a given value $\delta \in (0, \delta^*]$ (see Fig. 2(a)).
Case 2: $\bar{O}_i$ is on the boundary of the i-th MW-Voronoi region. Suppose $\bar{O}_i$ is on the curve ϵ. Since $\bar{O}_i$ and $T^{\bar{V}_{i1}}_{\Omega}$ are distinct for any $\Omega \in \mathbf{\Omega}_i$, one can choose a point $\hat{O}$ on ϵ such that $d(\hat{O}, \bar{V}_{i1}) > d(\bar{O}_i, \bar{V}_{i1})$ and the distance between $\bar{O}_i$ and $\hat{O}$ is equal to a given value $\delta \in (0, \delta^*]$ (see Fig. 2(b)).
In both cases, according to the triangle inequality:

$$d(\hat{O}, V) \geq d(\bar{O}_i, V) - \delta \geq \hat{u} - \delta, \quad \forall V \in \mathbf{V}_i - \{\bar{V}_{i1}\} \tag{3}$$

From the above relation and on nothing that $\hat{u} - \delta \geq \bar{r}_i + \delta > \bar{r}_i$ and $d(\hat{O}, \bar{V}_{i1}) > d(\bar{O}_i, \bar{V}_{i1})$, it can be concluded that

$$\min_{V \in \mathbf{V}_i} \left\{ d(\hat{O}, V) \right\} > \bar{r}_i, \quad i \in \mathbf{n} \tag{4}$$

which contradicts the initial assumption that $\bar{O}_i$ is the Maxmin-vertex centroid. This means that there is at least one more vertex on the Maxmin-vertex circle. ■

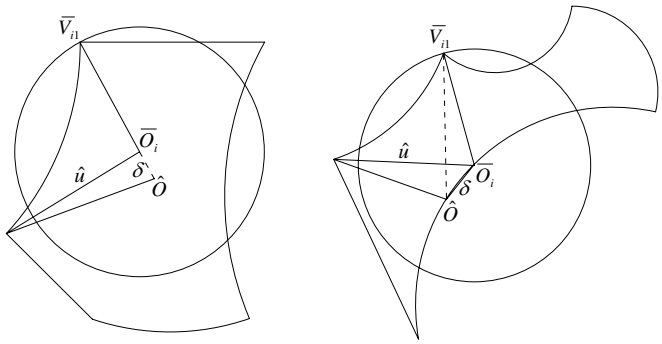

(a) (b)

Fig. 2: The Maxmin-vertex centroid, when it is: (a) inside an MW-Voronoi region, and (b) on the boundary of an MW-Voronoi region.

Lemma 2. *Given an MW-Voronoi diagram, assume that the Maxmin-vertex circle of one of the regions, say region i ($i \in \mathbf{n}$), passes through exactly two vertices $\bar{V}_{i1}$ and $\bar{V}_{i2}$. Then $\bar{O}_i$ is the intersection point of the perpendicular bisector of $\bar{V}_{i1}\bar{V}_{i2}$ and the boundary of the i-th MW-Voronoi region.*

Proof: Suppose $\bar{O}_i$ is not the intersection point of the boundary of the i-th MW-Voronoi region and the perpendicular bisector of $\bar{V}_{i1}\bar{V}_{i2}$, i.e., $\bar{O}_i$ is inside the i-th region. Define:

$$\tilde{u} := \min_{V \in \mathbf{V}_i - \{\bar{V}_{i1}, \bar{V}_{i2}\}} \left\{ d(\bar{O}_i, V) \right\}, \quad i \in \mathbf{n} \tag{5}$$

Since $\Omega(\bar{O}_i, \bar{r}_i)$ passes through exactly two vertices, thus $\delta^* = (\tilde{u} - \bar{r}_i)/2$ is strictly positive. Let $\tilde{O}$ be a point on the perpendicular bisector of $\bar{V}_{i1}\bar{V}_{i2}$ and outside the triangle $\bar{V}_{i1}\bar{V}_{i2}\bar{O}_i$, but closer to $\bar{O}_i$, such that the distance between the points $\bar{O}_i$ and $\tilde{O}$ is equal to a given value $\delta \in (0, \delta^*]$ (see Fig. 3). Using the triangle inequality, one can write:

$$d(\tilde{O}, V) \geq d(\bar{O}_i, V) - \delta \geq \tilde{u} - \delta, \quad \forall V \in \mathbf{V}_i - \{\bar{V}_{i1}, \bar{V}_{i2}\} \tag{6}$$

Using (6) along with the relations $\tilde{u}-\delta \geq \tilde{u}-\delta^* = \bar{r}_i+\delta^* > \bar{r}_i$

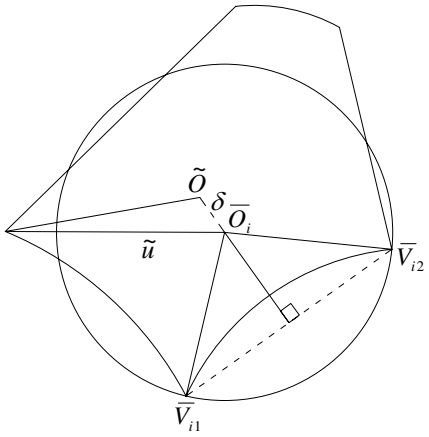

Fig. 3: An illustrative figure used in the proof of Lemma 2.

and $d(\tilde{O},\bar{V}_{i1}) = d(\tilde{O},\bar{V}_{i2}) > \bar{r}_i$, one arrives at:

$$\min_{V\in\mathbf{V}_i}\left\{d(\tilde{O},V)\right\} > \bar{r}_i, \quad i\in\mathbf{n} \tag{7}$$

which contradicts the initial assumption that $\bar{O}_i$ is the Maxmin-vertex centroid. This completes the proof. ■

Definition 7. For convenience of notation, the circle passing through two vertices V_p and V_q of region i in the MW-Voronoi diagram $\mathcal{V}$, centered at the intersection of the perpendicular bisector of V_pV_q and the boundary curve V_kV_l, is denoted by $\Omega^{k,l}_{p,q}$, $k,l,p,q \in \mathbf{m}_i$. Also, the circle passing through three vertices V_p, V_q and V_r of region i is denoted by $\Omega_{p,q,r}$, for $p,q,r\in\mathbf{m}_i$. In addition, the circle passing through one vertex V_r of MW-Voronoi region i, centered at $T^{V_r}_{\Omega}$, is denoted by $\Theta^{V_r}_{\Omega}$, for any $r\in\mathbf{m}_i$ and $\Omega\in\mathbf{\Omega}_i$.

Theorem 3. *Given an MW-Voronoi diagram, suppose the i-th region ($i\in\mathbf{n}$) has more than one boundary curve. Denote by $\hat{\mathbf{C}}_i$ and $\grave{\mathbf{C}}_i$ the sets of all circles $\Omega^{k,l}_{p,q}$, $\forall k,l,p,q\in\mathbf{m}_i$ and $\Theta^{V_r}_{\Omega}$, $\forall r\in\mathbf{m}_i$, $\Omega\in\mathbf{\Omega}_i$, respectively, centered on the boundary of the i-th region, and do not enclose any of the vertices of this region. Denote by $\tilde{\mathbf{C}}_i$ the set of all circumcircles of any three vertices, centered inside the i-th MW-Voronoi region or on its boundary, which do not enclose any of the vertices of this region. Define $\mathbf{C}_i = \hat{\mathbf{C}}_i\cup\grave{\mathbf{C}}_i\cup\tilde{\mathbf{C}}_i$. Then the circle $\Omega(\bar{O}_i,\bar{r}_i)$ belongs to $\mathbf{C}_i$, and it is the largest circle in this set.*

Proof: If $\Omega(\bar{O}_i,\bar{r}_i)\notin\grave{\mathbf{C}}_i$, then according to Lemma 1 the Maxmin-vertex circle passes through more than one vertex. If it passes through exactly two vertices, say V_1,V_2, then according to Lemma 2, there exist $k,l\in\mathbf{m}_i$ such that $\Omega(\bar{O}_i,\bar{r}_i)=\Omega^{k,l}_{1,2}$. Hence, in this case $\Omega(\bar{O}_i,\bar{r}_i)\in\mathbf{C}_i$, and from Definition 6, $\bar{r}_i = \max\{r\,|\Omega(O,r)\in\mathbf{C}_i\}$. If, on the other hand, the Maxmin-vertex circle passes through three or more Voronoi vertices, then it is the circumcircle of those vertices. Therefore, $\Omega(\bar{O}_i,\bar{r}_i)\in\mathbf{C}_i$, and again it is deduced from Definition 6 that $\bar{r}_i=\max\{r\,|\Omega(O,r)\in\mathbf{C}_i\}$. ■

C. Minmax-Vertex Strategy

The main idea of the Minmax-vertex method is that normally to achieve high area coverage, no sensor should be "too far" from any of its Voronoi vertices. The Minmax-vertex algorithm selects the target location of each sensor as a point inside its MW-Voronoi region with minimum distance from the farthest vertex. This point will be referred to as the *Minmax-vertex centroid*, and will be denoted by $\check{O}_i$ for the i-th region ($i\in\mathbf{n}$). Furthermore, the distance between this point and the farthest vertex from it in the i-th region will be represented by $\check{r}_i$. The Minmax-vertex circle is defined next.

Definition 8. The Minmax-vertex circle of an MW-Voronoi region is defined as the smallest circle centered inside the region such that all of the vertices of the region are either inside the circle or on it. This circle is, in fact, $\Omega(\check{O}_i,\check{r}_i)$, for the i-th region ($i\in\mathbf{n}$).

Lemma 3. *In the case when an MW-Voronoi region is not a circle (i.e., it has at least two boundary curves), its Minmax-vertex circle passes through more than one vertex.*

Proof: Let $\check{V}_{i1}$ be the farthest vertex to $\check{O}_i$ on the boundary of the i-th MW-Voronoi region, and define:

$$\hat{z} := \max_{V\in\mathbf{V}_i-\{\check{V}_{i1}\}}\left\{d(\check{O}_i,V)\right\}, \quad i\in\mathbf{n} \tag{8}$$

Suppose that the Minmax-vertex circle does not pass through any vertex other than $\check{V}_{i1}$, and hence $\delta^* = (\check{r}_i-\hat{z})/2$ is strictly positive. There are two possible cases, as discussed below.
Case 1: $\check{O}_i$ is inside the i-th MW-Voronoi region. Let $\hat{O}$ be a point inside the i-th MW-Voronoi region and on the line $\check{V}_{i1}\check{O}_i$ such that the distance between $\check{O}_i$ and $\hat{O}$ is equal to a given value $\delta\in(0,\delta^*]$ (see Fig. 4(a)).
Case 2: $\check{O}_i$ is on the boundary of the MW-Voronoi region. Suppose $\check{O}_i$ is on the curve ϵ. Let $\hat{O}$ be a point on ϵ or inside the i-th MW-Voronoi region such that $d(\hat{O},\check{V}_{i1}) < d(\check{O}_i,\check{V}_{i1})$, and the distance between $\check{O}_i$ and $\hat{O}$ is equal to a given value $\delta\in(0,\delta^*]$ (see Fig. 4(b)).
In both cases, according to the triangle inequality:

$$d(\hat{O},V)\leq d(\check{O}_i,V)+\delta\leq\hat{z}+\delta, \quad \forall V\in\mathbf{V}_i-\{\check{V}_{i1}\} \tag{9}$$

From the above relation and on noting that $\hat{z}+\delta\leq\check{r}_i-\delta<\check{r}_i$

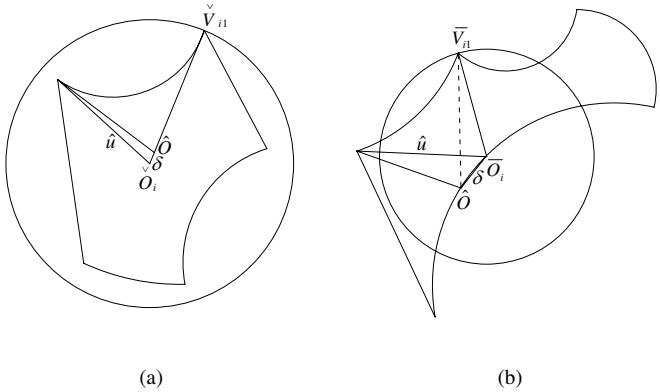

Fig. 4: Minmax-vertex centroid, when it is: (a) inside an MW-Voronoi region, and (b) on the boundary of an MW-Voronoi region.

and $d(\hat{O},\check{V}_{i1}) < d(\check{O}_i,\check{V}_{i1})$, it can be concluded that

$$\max_{V\in\mathbf{V}_i}\left\{d(\hat{O},V)\right\} < \check{r}_i, \ i\in\mathbf{n} \tag{10}$$

which contradicts the initial assumption that $\check{O}_i$ is the Minmax-vertex centroid. This means that there is at least one more

vertex on the Minmax-vertex circle. ■

Lemma 4. *Given an MW-Voronoi diagram, assume that the Minmax-vertex circle of one region, say region i ($i \in \mathbf{n}$), passes through exactly two vertices $\check{V}_{i1}$ and $\check{V}_{i2}$. Then $\check{O}_i$ is the intersection point of the perpendicular bisector of $\check{V}_{i1}\check{V}_{i2}$ and the boundary of the i-th MW-Voronoi region.*

Proof: Suppose $\check{O}_i$ is not the intersection point of the perpendicular bisector of $\check{V}_{i1}\check{V}_{i2}$ and the boundary of the i-th MW-Voronoi region, i.e., $\check{O}_i$ is inside the i-th region. Define:

$$\tilde{z} := \max_{V \in \mathbf{V}_i - \{\check{V}_{i1}, \check{V}_{i2}\}} \left\{ d(\check{O}_i, V) \right\}, \ i \in \mathbf{n} \tag{11}$$

Since $\Omega(\check{O}_i, \check{r}_i)$ passes through exactly two vertices, thus $\delta^* = (\check{r}_i - \tilde{z})/2$ is strictly positive. Let $\tilde{O}$ be a point on the perpendicular bisector of $\check{V}_{i1}\check{V}_{i2}$ and inside the triangle $\check{V}_{i1}\check{V}_{i2}\check{O}_i$, but closer to $\check{O}_i$, such that the distance between the points $\check{O}_i$ and $\tilde{O}$ is equal to a given value $\delta \in (0, \delta^*]$ (see Fig. 5). Using the triangle inequality, one can write:

$$d(\tilde{O}, V) \leq d(\check{O}_i, V) + \delta \leq \tilde{z} + \delta, \ \forall V \in \mathbf{V}_i - \{\check{V}_{i1}, \check{V}_{i2}\} \tag{12}$$

Using (12) along with the relations $\tilde{z} + \delta \leq \tilde{z} + \delta^* = \check{r}_i - \delta^* <$

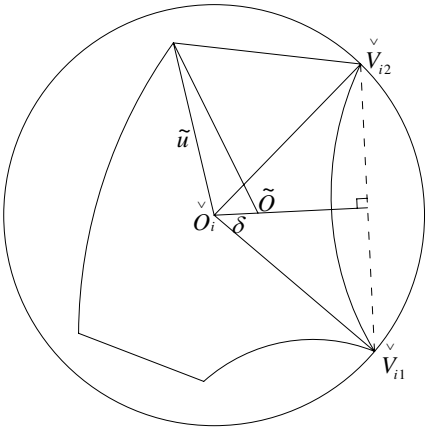

Fig. 5: An illustrative figure used in the proof of Lemma 4.

$\check{r}_i$ and $d(\tilde{O}, \check{V}_{i1}) = d(\tilde{O}, \check{V}_{i2}) < \check{r}_i$, one can conclude that:

$$\max_{V \in \mathbf{V}_i} \left\{ d(\tilde{O}, V) \right\} < \check{r}_i, \ i \in \mathbf{n} \tag{13}$$

which contradicts the initial assumption that $\check{O}_i$ is the Minmax-vertex centroid. This completes the proof. ■

Theorem 4. *Given an MW-Voronoi diagram, let $\hat{\mathbf{W}}_i$ be the set of all circles $\Omega^{k,l}_{p,q}$, $\forall k, l, p, q \in \mathbf{m}_i$, centered on the boundary of the i-th region, with all vertices of the region either inside the circles or on them. Let also $\tilde{\mathbf{W}}_i$ be the set of all circumcircles of any three vertices, centered inside or on the i-th region, with all vertices of the region either inside or on them. Define $\mathbf{W}_i := \hat{\mathbf{W}}_i \cup \tilde{\mathbf{W}}_i$. Then the circle $\Omega(\check{O}_i, \check{r}_i)$ belongs to $\mathbf{W}_i$, and it is the smallest circle in this set.*

Proof: According to Lemma 3, the Minmax-vertex circle passes through more than one Voronoi vertex. If it passes through no more than two Voronoi vertices, say V_{i1}, V_{i2}, then according to Lemma 4, there exist $k, l \in \mathbf{m}_i$ such that $\Omega(\check{O}_i, \check{r}_i) = \Omega^{k,l}_{1,2}$. Hence, in this case $\Omega(\check{O}_i, \check{r}_i) \in \mathbf{W}_i$, and from Definition 8, $\check{r}_i = \min\{r \,|\Omega(O, r) \in \mathbf{W}_i\}$. If, on the other hand, the Minmax-vertex circle passes through three or more Voronoi vertices, then it is the circumcircle of those vertices. Therefore, $\Omega(\check{O}_i, \check{r}_i) \in \mathbf{W}_i$, and again it is deduced from Definition 8 that $\check{r}_i = \min\{r \,|\Omega(O, r) \in \mathbf{W}_i\}$. ■

Remark 1. As noted in [17], when the sensing radii of the sensors are the same, the Voronoi regions turn out to be polygons. In this case, the smallest circle enclosing a polygon can be obtained by solving a rather simple convex optimization problem, and the center of the circle is called the *circumcenter* [18]. In the general case when the sensing radii of the sensors are not the same, however, the MW-Voronoi region boundaries are portions of the Apollonian circles and are not straight lines. Thus, the Maxmin-vertex and Minmax-vertex centroids cannot be obtained by the linear programming approach or other convex optimization methods. Theorems 3 and 4 use an efficient geometric approach in this case to find the centroids.

Remark 2. According to Theorems 2, 3 and 4, the complexity of the algorithms to find the new location of the i-th sensor in the FPB strategy is of order $O(m_i)$, while it is of order $O(m_i^4)$ in the Minmax-vertex and Maxmin-vertex algorithms. In addition, regardless of the number of sensors, their sensing and communication capabilities, field size, etc., the MW-Voronoi diagrams partition the field in such a way that the number of vertices of each region is typically not "too large". Hence, the problem of finding the new location of the sensors is usually not too complex, computationally.

Theorem 5. *The proposed algorithms (FPB, Minmax-vertex and Maxmin-vertex) are convergent.*

Proof: Let the positions and sensing radii of the sensors in the k-th round be denoted by $\mathbf{P}(k) = \{P_1(k), P_2(k), \ldots, P_n(k)\}$ and $\mathbf{r}(k) = \{r_1(k), r_2(k), \ldots, r_n(k)\}$, respectively. Denote also the MW-Voronoi regions in the k-th round by $\Pi_1(k), \Pi_2(k), \ldots, \Pi_n(k)$, and the corresponding total covered area of the field by $\beta(k)$. If the k-th round is not the final round, then some sensors move and change their locations in the next round. Assume that the i-th sensor, $i \in \mathbf{n}$, moves to the new location $P_i(k+1) \neq P_i(k)$; if the coverage area w.r.t. this location is greater than the previous local coverage area, i.e. $\beta^{P_i(k+1)}_{\Pi_i(k)} > \beta^{P_i(k)}_{\Pi_i(k)}$, then according to Theorem 1 the total coverage in the network increases in this round, i.e. $\beta(k+1) > \beta(k)$. On the other hand, the total covered area is upper-bounded by the overall area of the field, from which the convergence of the algorithms is implied. ■

Remark 3. The convergence of the proposed sensor coordination algorithms is implied from the results obtained. However, the convergence may not be achieved in finite time.

To terminate the algorithms in finite time, an appropriate threshold ϵ is considered for the minimum acceptable coverage increase as noted earlier, such that the algorithm will continue after the k-th round only if there is a sensor in the network whose coverage increases at least by ϵ in the following iteration, i.e. $\exists i \in \mathbf{n} : \beta^{P_i(k+1)}_{\Pi_i(k)} \geq \beta^{P_i(k)}_{\Pi_i(k)} + \epsilon$. Note that the choice of ϵ involves a trade-off between network coverage and deployment time. The following theorem (along with its proof) is borrowed from [17], and provides an upper-bound on the

number of rounds required to run the algorithm, as a function of ϵ.

Theorem 6. *Consider a set of n mobile sensors $\mathbf{S}$, randomly deployed in a 2D field. Using any of the proposed algorithms with the coverage improvement threshold ϵ, the number of required rounds to run the algorithm is at most $\frac{A_{total}}{\epsilon}$, where A_{total} is the overall area of the field.*

Proof: Let the number of rounds required to run the algorithm in order to meet the termination condition be denoted by ζ_f. Let also the total uncovered area of the field in the k-th round be represented by $\theta(k)$, and note that $\beta(k) = A_{total} - \theta(k)$. Denote the position of the sensors and their corresponding MW-Voronoi regions in the k-th round by $\mathbf{P}(k) = \{P_1(k), P_2(k), \ldots, P_n(k)\}$ and $\Pi_1(k), \Pi_2(k), \ldots, \Pi_n(k)$, respectively. It is concluded from the properties of the MW-Voronoi diagram that:

$$\theta(k) = \sum_{i=1}^{n} \theta_{\Pi_i(k)}^{P_i(k)}, \ \forall 1 \leq k \leq \zeta_f \tag{14}$$

Define the *moving set of the k-th round* as the largest subset of $\mathbf{S}$ that moves in the k-th round, and denote the indices of the sensors in this set by $\mathbf{Indx}(k)$. Note that at least one sensor moves in the k-th round, i.e. $\mathbf{Indx}(k) \neq \emptyset$, $\forall 1 \leq k \leq \zeta_f$. Note also that the i-th sensor, $i \in \mathbf{Indx}(k)$, moves in the k-th round if $\beta_{\Pi_i(k)}^{P_i(k+1)} \geq \beta_{\Pi_i(k)}^{P_i(k)} + \epsilon$. This means that:

$$\theta_{\Pi_i(k)}^{P_i(k+1)} \leq \theta_{\Pi_i(k)}^{P_i(k)} - \epsilon, \quad \forall i \in \mathbf{Indx}(k) \tag{15}$$

On the other hand, it is possible that some of the points in $\theta_{\Pi_i(k)}^{P_i(k+1)}$ are also covered by another sensor located at $P_j(k+1)$, for some $j \in \mathbf{n}\backslash\{i\}$. Hence:

$$\theta(k+1) \leq \sum_{i=1}^{n} \theta_{\Pi_i(k)}^{P_i(k+1)} \tag{16}$$

Since for any $i \in \mathbf{n}\backslash\mathbf{Indx}(k)$ the i-th sensor does not move (which implies $\theta_{\Pi_i(k)}^{P_i(k+1)} = \theta_{\Pi_i(k)}^{P_i(k)}$), from (15) and (16) one arrives at:

$$\theta(k+1) \leq \sum_{i=1}^{n} \theta_{\Pi_i(k)}^{P_i(k)} - |\mathbf{Indx}(k)|\,\epsilon \tag{17}$$

It is now concluded from (14) and (17) that:

$$\theta(k+1) \leq \theta(k) - |\mathbf{Indx}(k)|\,\epsilon \leq \theta(k) - \epsilon \tag{18}$$

or equivalently:

$$\beta(k+1) \geq \beta(k) + |\mathbf{Indx}(k)|\,\epsilon \geq \beta(k) + \epsilon \tag{19}$$

which means that using the proposed sensor coordination scheme, in each round the total covered area increases by at least ϵ. Therefore, the total amount of increased coverage from the first round to the termination round is greater than or equal to $\zeta_f \epsilon$. Since the total covered area is always less than or equal to A_{total}, hence $A_{total} \geq \zeta_f \epsilon$ or equivalently $\frac{A_{total}}{\epsilon} \geq \zeta_f$. ■

Remark 4. One of the important properties of the MW-Voronoi diagram is that first of all it partitions the field, and more importantly there is exactly one sensor in each region. Since the new location of every sensor under the algorithms developed in this work is inside its own MW-Voronoi region and the sensor moves only within the region, collision will never occur. Note that if some sensors could not communicate with their neighbors, then the MW-Voronoi region constructed around each one of them might be wrong. Consequently, not only does this have a negative impact on the detection of coverage holes, it could also lead to sensor collision.

IV. Simulation Results

Example 1: In this example, the three algorithms developed in the previous section are applied to a $50\text{m} \times 50\text{m}$ flat space. In each simulation, the algorithm continues as long as the coverage area of at least one of the sensors in its MW-Voronoi region increases by more than 0.1m^2 in the next move, and is terminated otherwise. The results are obtained by performing 20 simulations with different random initial locations for the sensors.

Assume first 27 sensors are randomly deployed in a $50\text{m} \times 50\text{m}$ plane: 15 with a sensing radius of 6m, 6 with a sensing radius of 5m, 3 with a sensing radius of 7m, and 3 with a sensing radius of 9m. Moreover, the communication range of each sensor is assumed to be $10/3$ times greater than its sensing range. The coverage factor (defined as the ratio of the covered area to the overall area) of the sensors in each round is depicted in Fig. 9 for the three algorithms proposed in this paper. It can be observed from this figure that all three strategies result in a satisfactory coverage level of the sensing field in the first few rounds of the corresponding algorithms. The resultant curves also show that the Minmax-vertex algorithm performs better than the other algorithms as far as coverage is concerned.

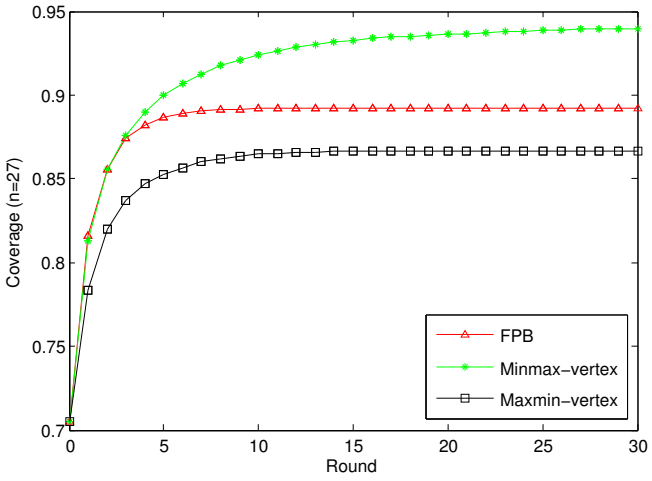

Fig. 6: Covered area percentage per round for 27 sensors.

It is desired now to compare the performance of the proposed algorithms in terms of the number of deployed sensors n. To this end, consider three more setups: n=18, 36, and 45 (in addition to n=27 discussed above). Let changes in the number of identical sensors in the new setups be proportional to the changes in the total number of sensors (e.g., for the case of n=18 there will be 10 sensors with a sensing radius of 6m, 4 with a sensing radius of 5m, 2 with a sensing radius of 7m, and 2 with a sensing radius of 9m). Fig. 7 provides the coverage results for different number of sensors. It can be seen from this figure that the covered area under the Minmax-vertex algorithm is greatet than that under other algorithms for different number of sensors.

The convergence rate of sensors in reaching the steady-state coverage level is also an important measure of the efficiency of

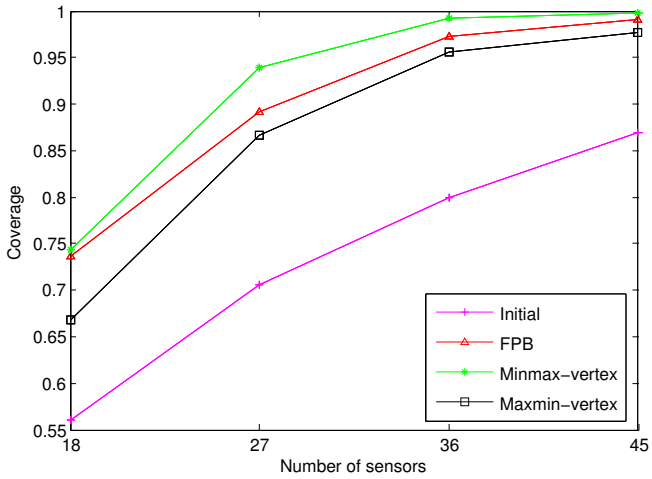

Fig. 7: Network coverage for different number of sensors using the proposed algorithms.

sensor coordination algorithms. Since the sensor deployment time of all algorithms is more or less the same in each round, in Fig. 8 the number of rounds required to reach the steady state (i.e., to satisfy the termination condition specified earlier) are shown to evaluate the convergence speed of different algorithms.

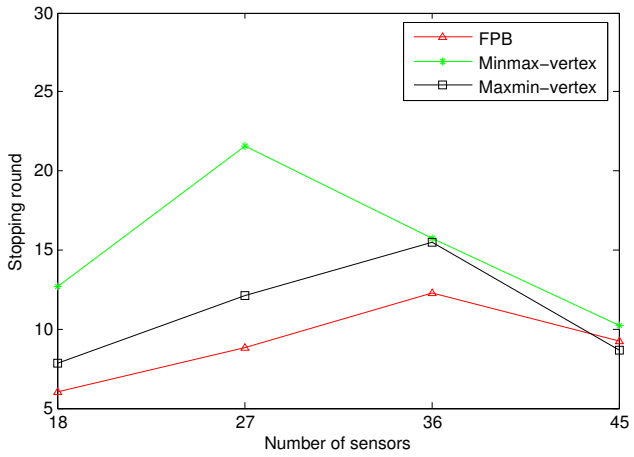

Fig. 8: The number of rounds required to reach the termination conditions for different number of sensors using the proposed algorithms.

Another important means of assessing the performance of the sensor deployment algorithms is energy efficiency. The consumed movement energy of each sensor is known to be directly related to its traveling distance, as well as the number of times it stops (the latter is related to the static friction). Thus, to compare the energy efficiency of the proposed techniques, the traveling distance and the number of movements should be taken into consideration. To evaluate the energy efficiency of the algorithms, assume that the movement energy of each sensor is 0.210J/inch (or 8.268J/m) [19], [20]. In other words, the energy required to move a sensor by 1 inch (without stopping) is 0.210J. Consider two scenarios, where the energy required for bringing a sensor to a complete stop and then moving it by overcoming the static friction instantaneously is equal to (i) 8.268J, and (ii) 33.072J [10], [21]. Tables I and II provide a summary of the energy consumption results for these two cases. Define α as the ratio of energy consumption due to one stop followed by one move from complete stop to energy consumption due to one meter move. Now, if there are a large number of sensors in the field and the power required to overcome static friction of a sensor is much larger than that required to move it (per unit), the Maxmin-vertex algorithm is more energy-efficient than the other two algorithms. If, however, the power required to overcome static friction of a sensor is much smaller than that required to move it, then regardless of the number of sensors the FPB algorithm performs better than the other two algorithms in terms of energy consumption.

The above discussion is summarized below (logic and's in these statements are capitalized):

1) The Minmax-vertex algorithm performs better in terms of network coverage.
2) The Maxmin-vertex algorithm outperforms the other two algorithms when there are a large number of sensors in the field, AND:
   - the deployment time is the main concern.
   - the energy consumption is the main concern, AND the power required to overcome the static friction of a sensor is much larger than that required to move it (per unit).
3) The FPB algorithm is more desirable when:
   - the deployment time is the main concern AND the number of sensors in the field is not large.
   - the energy consumption is the main concern, AND the power required to overcome the static friction of a sensor is much smaller than that required to move it (per unit).
   - the computational complexity is concerned.

Example 2: Consider 36 sensors distributed randomly in a 50m by 50m field. Assume 20 of these sensors have a communication range of 20m, 8 have a communication range of 16.66m, 4 have a communication range of 30m, and 4 have a communication range of 23.33m. The sensing radius of each sensor is assumed to be 33% of its communication radius. It is desired now to compare the three algorithms developed in this paper with some other methods presented in [17], namely the WVB, Minmax-curve and Maxmin-curve algorithms. The coverage factor in every round of each algorithm is provided in Figure 9. It can be observed from this figure that the Minmax-vertex and FPB algorithms outperform the other algorithms in terms of coverage factor.

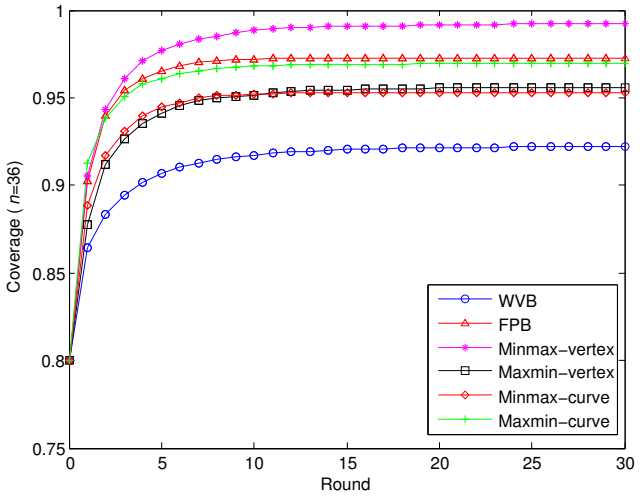

Fig. 9: Coverage factor in each round of different algorithms in Example 2.

TABLE I: The energy consumption in Joule for different number of sensors using the proposed algorithms for the first scenario of Example 1

	$n = 18$	$n = 27$	$n = 36$	$n = 45$
FPB	47.4234 J	44.7480 J	42.9542 J	28.1041 J
Minmax-vertex	77.6335 J	95.0093 J	68.6495 J	37.0676 J
Maxmin-vertex	50.9095 J	56.8741 J	48.2570 J	27.3611 J

TABLE II: The energy consumption in Joule for different number of sensors using the proposed algorithms for the second scenario of Example 1

	$n = 18$	$n = 27$	$n = 36$	$n = 45$
FPB	83.8715 J	97.3876 J	105.4810 J	71.0150 J
Minmax-vertex	153.3546 J	232.9012 J	163.1114 J	84.8015 J
Maxmin-vertex	83.8437 J	115.5310 J	105.1340 J	58.4763 J

Remark 5. Note that the size of the field and the number of sensors considered in this section are more or less the same as the ones used in the literature (e.g., see [10], [22], [23], [24], [25]). Moreover, the sensing and communication ranges of sensors considered in the simulations are consistent with the setting used in [10], [26] and other sensor prototypes such as Smart Dust, CTOS dust, and Wins (Rockwell) [21].

V. Conclusions

Efficient sensor coordination algorithms are developed in this work to increase sensing coverage in a network of mobile sensors with non-identical sensing ranges. The sensing field is first partitioned using the multiplicatively weighted Voronoi (MW-Voronoi) diagram, and three distributed deployment algorithms are subsequently developed. Under the proposed algorithms, the sensors move iteratively in such a way that coverage holes are reduced in size. The algorithms tend to move the sensors in proper directions such that the network configuration (in terms of the distance of sensors from the vertices of the MW-Voronoi regions) becomes closer to an ideal configuration. To avoid complex non-convex optimization problems, novel geometric methods are used to find the new sensor locations in the MW-Voronoi regions. The proposed algorithms are compared with other techniques with different number of sensors.

References

[1] Z. Zou, Y. Bao, H. Li, B. F. Spencer, and J. Ou, "Embedding compressive sensing-based data loss recovery algorithm into wireless smart sensors for structural health monitoring," *IEEE Sensors Journal*, vol. 15, no. 2, pp. 797–808, 2015.

[2] X. Wang, S. Han, Y. Wu, and X. Wang, "Coverage and energy consumption control in mobile heterogeneous wireless sensor networks," *IEEE Transactions on Automatic Control*, vol. 58, no. 4, pp. 975–988, 2013.

[3] S. Zhu and Z. Ding, "Distributed cooperative localization of wireless sensor networks with convex hull constraint," *IEEE Transactions on Wireless Communications*, vol. 10, no. 7, pp. 2150–2161, 2011.

[4] M. Pourali and A. Mosleh, "A functional sensor placement optimization method for power systems health monitoring," *IEEE Transactions on Industry Applications*, vol. 49, no. 4, pp. 1711–1719, 2013.

[5] H. Mahboubi, W. Masoudimansour, A. G. Aghdam, and K. Sayrafian-Pour, "Maximum lifetime strategy for target monitoring with controlled node mobility in sensor networks with obstacles," *IEEE Transactions on Automatic Control*, vol. 61, no. 11, pp. 3493–3508, 2016.

[6] S. Fang, L. D. Xu, Y. Zhu, J. Ahati, H. Pei, J. Yan, and Z. Liu, "An integrated system for regional environmental monitoring and management based on internet of things," *IEEE Transactions on Industrial Informatics*, vol. 10, no. 2, pp. 1596–1605, 2014.

[7] H. Mahboubi, A. Momeni, A. G. Aghdam, K. Sayrafian-Pour, and V. Marbukh, "An efficient target monitoring scheme with controlled node mobility for sensor networks," *IEEE Transactions on Control Systems Technology*, vol. 20, no. 6, pp. 1522–1532, 2012.

[8] H. Mahboubi, K. Moezzi, A. G. Aghdam, and K. Sayrafian-Pour, "Self-deployment algorithms for field coverage in a network of nonidentical mobile sensors: Vertex-based approach," in *Proceedings of American Control Conference*, 2011, pp. 3227–3232.

[9] A. Howard, M. J. Matarić, and G. S. Sukhatme, "An incremental self-deployment algorithm for mobile sensor networks," *Autonomous Robots*, vol. 13, no. 2, pp. 113–126, 2002.

[10] G. Wang, G. Cao, and T. F. L. Porta, "Movement-assisted sensor deployment," *IEEE Transactions on Mobile Computing*, vol. 5, no. 6, pp. 640–652, 2006.

[11] I. Dietrich and F. Dressler, "On the lifetime of wireless sensor networks," *ACM Transactions on Sensor Networks*, vol. 5, no. 1, pp. 1–39, 2009.

[12] E. Deza and M. M. Deza, *Encyclopedia of Distances*. Springer, 2009.

[13] H. Mahboubi, K. Moezzi, A. G. Aghdam, K. Sayrafian-Pour, and V. Marbukh, "Distributed deployment algorithms for improved coverage in a network of wireless mobile sensors," *IEEE Transactions on Industrial Informatics*, vol. 10, no. 1, pp. 163–174, 2014.

[14] A. V. Akopyan and A. A. Zaslavsky, *Geometry of Conics*. American Mathematical Society, 2007.

[15] A. Kwok and S. Martinez, "A distributed deterministic annealing algorithm for limited-range sensor coverage," *IEEE Transactions on Control Systems Technology*, vol. 19, no. 4, pp. 792–804, 2011.

[16] H. Mahboubi, J. Habibi, A. G. Aghdam, and K. Sayrafian-Pour, "Distributed deployment strategies for improved coverage in a network of mobile sensors with prioritized sensing field," *IEEE Transactions on Industrial Informatics*, vol. 9, no. 1, pp. 451–461, 2013.

[17] H. Mahboubi, K. Moezzi, A. G. Aghdam, and K. Sayrafian-Pour, "Distributed deployment algorithms for efficient coverage in a network of mobile sensors with nonidentical sensing capabilities," *IEEE Transactions on Vehicular Technology*, vol. 63, no. 8, pp. 3998–4016, 2014.

[18] S. P. Boyd and L. Vandenberghe, *Convex Optimization*. Cambridge University Press, 2004.

[19] S. Yoon, O. Soysal, M. Demirbas, and C. Qiao, "Coordinated locomotion and monitoring using autonomous mobile sensor nodes," *IEEE Transactions on Parallel and Distributed Systems*, vol. 22, no. 10, pp. 1742–1756, 2011.

[20] M. Rahimi, H. Shah, G. S. Sukhatme, J. Heideman, and D. Estrin, "Studying the feasibility of energy harvesting in a mobile sensor network," in *Proceedings of IEEE International Conference on Robotics and Automation*, vol. 1, 2003, pp. 19–24.

[21] G. Wang, G. Cao, P. Berman, and T. F. L. Porta, "A bidding protocol for deploying mobile sensors," *IEEE Transactions on Mobile Computing*, vol. 6, no. 5, pp. 563–576, 2007.

[22] A. Galllais, J. Carle, D. Simplot-Ryl, and I. Stojmenovic, "Localized sensor area coverage with low communication overhead," *IEEE Transactions on Mobile Computing*, vol. 7, no. 5, pp. 661–672, 2008.

[23] R. S. Chang and S. H. Wang, "Self-deployment by density control in sensor networks," *IEEE Transactions on Vehicular Technology*, vol. 57, no. 3, pp. 1745–1755, 2008.

[24] C. H. Caicedo-Nez and M. Zefran, "Distributed task assignment in mobile sensor networks," *IEEE Transactions on Automatic Control*, vol. 56, no. 10, pp. 2485–2489, 2011.

[25] K. Ma, Y. Zhang, and W. Trappe, "Managing the mobility of a mobile sensor network using network dynamics," *IEEE Transactions on Parallel and Distributed Systems*, vol. 19, no. 1, pp. 106–120, 2008.

[26] "Berkeley sensor and actuator center." [Online]. Available: http://www-bsac.eecs.berkeley.edu